

ARTICLES

Quantum instanton approximation for thermal rate constants of chemical reactionsWilliam H. Miller,^{a)} Yi Zhao, Michele Ceotto, and Sandy Yang*Department of Chemistry and Kenneth S. Pitzer Center for Theoretical Chemistry, University of California, and Chemical Sciences Division, Lawrence Berkeley National Laboratory, Berkeley, California 94720*

(Received 10 March 2003; accepted 15 April 2003)

A quantum mechanical theory for chemical reaction rates is presented which is modeled after the [semiclassical (SC)] instanton approximation. It incorporates the desirable aspects of the instanton picture, which involves only properties of the (SC approximation to the) Boltzmann operator, but corrects its quantitative deficiencies by replacing the SC approximation for the Boltzmann operator by the quantum Boltzmann operator, $\exp(-\beta\hat{H})$. Since a calculation of the quantum Boltzmann operator is feasible for quite complex molecular systems (by Monte Carlo path integral methods), having an accurate *rate* theory that involves only the Boltzmann operator could be quite useful. The application of this *quantum instanton* approximation to several one- and two-dimensional model problems illustrates its potential; e.g., it is able to describe thermal rate constants accurately ($\sim 10\text{--}20\%$ error) from high to low temperatures deep in the tunneling regime, and applies equally well to asymmetric and symmetric potentials. © 2003 American Institute of Physics.

[DOI: 10.1063/1.1580110]

I. INTRODUCTION

The calculation of thermal rate constants, $k(T)$, for chemical reactions remains one of the central tasks of theoretical chemistry. Within the Born–Oppenheimer (BO) approximation, a rigorous calculation of $k(T)$ requires that one solve the (quantum) dynamics for nuclear motion on the appropriate BO potential energy surface [for example, to construct a flux time correlation function which yields the rate constant; cf. Eq. (1.1)]. There are of course a variety of approximate ways for treating the nuclear dynamics that are useful in various circumstances: for example, if the temperature is high enough, then classical mechanics (perhaps with a quantum distribution of initial conditions¹) does a very good job. At lower temperature, the transition state theory (TST)^{2–4} assumption that no trajectories recross some dividing surface separating reactant and product coordinate space is usually valid, but here tunneling effects may be important so that a quantized version of TST is needed. Since TST is inherently a classical theory, there is no absolutely unambiguous way to quantize it, though many approximate approaches have been useful.^{5–13}

Our goal in this paper is to develop a more accurate and less *ad hoc* (i.e., more nearly “*ab initio*”) quantum version of TST, with a specific focus on the tunneling regime where quantum effects are most important, but which is also simple enough that it can be applied to systems with many degrees of freedom. To this end, we first recall a semiclassical (SC) TST¹⁴ that was presented by one of us many years ago, which became better known as the *instanton*^{15,16} approxima-

tion; the SC-TST, or instanton result, was obtained from the following rigorous quantum expression⁵ for the rate in terms of a flux correlation function,

$$k(T) = Q_r(T)^{-1} \lim_{t \rightarrow \infty} \text{tr} [e^{-\beta\hat{H}/2} \hat{F} e^{-\beta\hat{H}/2} e^{i\hat{H}t/\hbar} h e^{-i\hat{H}t/\hbar}], \quad (1.1)$$

by making a short time approximation for the time evolution operators (i.e., the assumption of TST-like dynamics), using the SC approximation for the Boltzmann operator¹⁷ (which involves classical trajectories in pure imaginary time, or equivalently, in real time on the upside-down potential energy surface), and evaluating the trace also semiclassically (i.e., via the stationary phase approximation). [In Eq. (1.1) $Q_r(T)$ is the reactant partition function per unit volume, \hat{F} the flux operator with respect to a dividing surface separating reactants and products, h a Heaviside function that is 1(0) on the product (reactant) side of a dividing surface, $\beta = 1/k_B T$, and \hat{H} the Hamiltonian operator of the molecular system.] The instanton result for the rate constant has many qualitatively correct and desirable features: e.g., there is no *ad hoc* assumption of a tunneling path, but rather it is determined by the dynamics on the full (multidimensional) potential energy surface (as the periodic classical trajectory on the upside-down potential energy surface) and correctly shows, for example, “corner-cutting” effects^{18–22} due to reaction path curvature. The tunneling factor involves the classical action along this periodic trajectory and is a natural generalization of the WKB tunneling probability for one dimension; the “frequencies of the activated complex” of standard TST emerge naturally, as the stability frequencies associated with the periodic orbit (and thus show coupling effects between

^{a)}Electronic mail: miller@cchem.berkeley.edu

the reaction coordinate and the degrees of freedom orthogonal to it). All of the ingredients of the rate constant are determined solely by the SC approximation to the Boltzmann operator. One may thus say that, within the SC approximation, the instanton approximation is the rigorous result for the TST rate constant.

The instanton approximation has been widely used to describe tunneling phenomena in a variety of processes in chemistry and condensed matter physics.^{16,23–25} Unfortunately, however, in application to perhaps the most elementary realistic model for a chemical reaction (collinear $\text{H} + \text{H}_2 \rightarrow \text{H}_2 + \text{H}$) it was seen²⁶ to be of only semiquantitative accuracy. (The analysis in Ref. 26 suggests that the problem is the local quadratic approximation about the instanton periodic orbit, which is inherent to the SC calculation.) To obtain quantitative results, one thus needs a more accurate treatment. The idea of the present work is to seek an instanton-like description but one expressed in terms of the *quantum* Boltzmann operator, $\exp(-\beta\hat{H})$, rather than its SC approximation (and also without the SC approximation to the trace). The hypothesis is that this should correct the major quantitative defects resulting from the SC aspects of the instanton approximation, while still retaining the simplifications inherent to the dynamical picture. And from a practical point of view, the evaluation of the quantum Boltzmann operator by Monte Carlo path integral methods is readily doable nowadays for quite large molecular systems, and probably no more difficult than it would be to find the instanton periodic orbit for such systems. There will be no tunneling path in this *quantum instanton* (QI) approximation, but the rate constant will be expressed wholly in terms of the quantum Boltzmann operator (which for complex systems can be evaluated by Monte Carlo path integral).

In Sec. II we first present the derivation of the quantum instanton (QI) approximation for one-dimensional systems, and show some numerical results for the standard Eckart potential barrier. It is important that this QI approximation is accurate for an asymmetric as well as a symmetric barrier. In Sec. III we present the generalization to multidimensional systems and show numerical results for the collinear $\text{H} + \text{H}_2$ and $\text{D} + \text{H}_2$ reactions. The results all indicate the QI approximation to be extremely accurate for the low temperature tunneling region for which it is designed, and (perhaps surprisingly) also of good accuracy at high temperature. It is equally well-defined for asymmetric and symmetric potential barriers. It does, however, still embody the TST assumption of a “direct” reaction mechanism and thus cannot describe aspects of the dynamics that involve recrossing flux.

In concluding this Introduction it is appropriate to note some other quantum versions of TST that have been presented and found utility for various purposes. First, there is more or less standard TST, including the variational choice of the best TS dividing surface, with semiclassical (WKB) tunneling corrections computed along some assumed path [adiabatic, sudden (i.e., straight line), etc.]; the treatment often uses a local harmonic approximation about the minimum energy path to characterize the potential energy surface and the “reaction path Hamiltonian”²⁷ to describe the curvature-induced coupling between the reaction coordinate and modes

orthogonal to it. Truhlar, Garrett, and co-workers²⁸ have developed such approaches extensively, calibrating the various approximations to accurate quantum results for simple systems and then incorporating judicious empiricism, to make a very useful overall package.²⁹ Voth *et al.*^{8,30} have also presented several versions of quantum TST that involve the quantum Boltzmann operator; one version invokes various short time approximations for the real time propagators in Eq. (1.1),³⁰ while another is based on the (thermally averaged) centroid of the path⁸ (in a path integral evaluation of the Boltzmann operator). The former of these is very closely related to the “linearized” version^{1,31} of the SC initial value representation (IVR) for the rate constant and Pollak’s recent quantum version of TST.^{13,32} There are a number of other TST-like approximations that are based on an (numerical) analytic continuation of the short time behavior of the flux–flux autocorrelation function: cf. the work by Yamasita and Miller,³³ Tromp and Miller,⁷ Andersen *et al.*,^{11,12} and most recently that by Krilov *et al.*^{34,35}

II. QUANTUM INSTANTON FOR 1D SYSTEMS

A. Derivation

We start with a formally exact expression for the rate constant in which the time has been integrated out,³⁶

$$k(T)Q_r(T) \equiv kQ_r = \frac{1}{2\pi\hbar} \int dE e^{-\beta E} \frac{1}{2} (2\pi\hbar)^2 \times \text{tr}[\hat{F}_1 \delta(E - \hat{H}) \hat{F}_2 \delta(E - \hat{H})], \quad (2.1)$$

where we have also taken the generalized case for which the two flux operators, \hat{F}_1 and \hat{F}_2 , may correspond to two different dividing surfaces [actually a “dividing point” in this one-dimensional (1D) case]; i.e.,

$$\hat{F}_n = \frac{1}{2m} [\delta(\hat{x} - x_n) \hat{p} + \hat{p} \delta(\hat{x} - x_n)], \quad (2.2a)$$

for $n=1,2$, and where \hat{p} is the momentum operator,

$$\hat{p} = \frac{\hbar}{i} \frac{\partial}{\partial x}; \quad (2.2b)$$

for definiteness, we take $x_1 < x_2$. Equation (2.1) gives the exact rate for any values of x_1 and x_2 , i.e., for any location of the two dividing surfaces. Evaluating the trace in a coordinate representation gives the following more explicit expression:

$$kQ_r = 2\pi\hbar \left(\frac{\hbar}{2m}\right)^2 \int dE e^{-\beta E} [\langle x_1 | \delta(E - \hat{H}) | x_2 \rangle' \times \langle x_2 | \delta(E - \hat{H}) | x_1 \rangle - \langle x_1 | \delta(E - \hat{H}) | x_2 \rangle \langle x_2 | \delta(E - \hat{H}) | x_1 \rangle], \quad (2.3)$$

where the prime on a bra or ket indicates differentiation with respect to the coordinate variable, i.e.,

$$\langle x_1 | \delta(E - \hat{H}) | x_2 \rangle = \frac{\partial}{\partial x_1} \langle x_1 | \delta(E - \hat{H}) | x_2 \rangle,$$

$$\langle x_1 | \delta(E - \hat{H}) | x_2 \rangle' = \frac{\partial^2}{\partial x_1 \partial x_2} \langle x_1 | \delta(E - \hat{H}) | x_2 \rangle.$$

For reasons that will be clear below, we choose the values of x_1 and x_2 such that

$$\langle x_1 | \delta(E - \hat{H}) | x_2 \rangle = 0, \tag{2.4a}$$

$$\langle x_1 | \delta(E - \hat{H}) | x_2 \rangle' = 0, \tag{2.4b}$$

i.e., so that the point (x_1, x_2) is an extremum in this two-dimensional (2D) space. Equation (2.3) for the rate constant can then be written as

$$kQ_r = 2\pi\hbar \left(\frac{\hbar}{2m}\right)^2 \frac{1}{2} \frac{\partial^2}{\partial x_1 \partial x_2} \int dE e^{-\beta E} \times (\langle x_2 | \delta(E - \hat{H}) | x_1 \rangle)^2. \tag{2.5}$$

The above discussion is still formally exact. We now wish to express the matrix elements of the microcanonical density operator, $\langle x_2 | \delta(E - \hat{H}) | x_1 \rangle$, in terms of those of the Boltzmann operator. As is well known, the exact relation between the two is that of a Laplace transform,

$$\langle x_2 | \delta(E - \hat{H}) | x_1 \rangle = \frac{1}{4\pi i} \int_{\gamma-i\infty}^{\gamma+i\infty} d\beta e^{\beta E/2} \langle x_2 | e^{-\beta \hat{H}/2} | x_1 \rangle, \tag{2.6}$$

where (for reasons that will be clear below) we have taken the integration variable to be $\beta/2$ rather than β . Motivated by semiclassical considerations (cf. Appendix A), we evaluate the integral over β by the steepest descent approximation (= the stationary phase approximation when the “phase” is pure imaginary). The result of this approximation, the details of which are given in Appendix A, is

$$\langle x_2 | \delta(E - \hat{H}) | x_1 \rangle = \frac{1}{\sqrt{2\pi\Delta H(\beta_0)}} e^{\beta_0 E/2} \langle x_2 | e^{-\beta_0 \hat{H}/2} | x_1 \rangle, \tag{2.7a}$$

where $\beta_0(E)$ is determined by the relation

$$E = E(\beta_0), \tag{2.7b}$$

with $E(\beta)$ defined by

$$E(\beta) \equiv -2 \frac{\partial}{\partial \beta} \log \langle x_2 | e^{-\beta \hat{H}/2} | x_1 \rangle = \langle x_2 | e^{-\beta \hat{H}/2} \hat{H} | x_1 \rangle / \langle x_2 | e^{-\beta \hat{H}/2} | x_1 \rangle, \tag{2.7c}$$

and where

$$\Delta H(\beta)^2 \equiv -2E'(\beta) = \frac{\langle x_2 | e^{-\beta \hat{H}/2} \hat{H}^2 | x_1 \rangle}{\langle x_2 | e^{-\beta \hat{H}/2} | x_1 \rangle} - \left(\frac{\langle x_2 | e^{-\beta \hat{H}/2} \hat{H} | x_1 \rangle}{\langle x_2 | e^{-\beta \hat{H}/2} | x_1 \rangle} \right)^2. \tag{2.7d}$$

Note, as discussed in Appendix A, that the $E \leftrightarrow \beta$ relation is unique if x_1 and x_2 are chosen as specified by Eq. (2.4). Utilizing Eq. (2.7a), Eq. (2.5) for the rate constant becomes

$$kQ_r = 2\pi\hbar \left(\frac{\hbar}{2m}\right)^2 \frac{1}{2} \frac{\partial^2}{\partial x_1 \partial x_2} \int dE e^{-\beta E} \times \frac{e^{\beta_0 E}}{2\pi\Delta H(\beta_0)^2} (\langle x_2 | e^{-\beta_0 \hat{H}/2} | x_1 \rangle)^2, \tag{2.8}$$

and the integral over E is now also to be evaluated by the steepest descent approximation. (That is, we have used the steepest descent approximation to go from β to E , and now to go from E to β !) The specifics of this are also given in Appendix A; utilizing Eqs. (A13)–(A16), Eq. (2.8) for the rate becomes

$$kQ_r = \frac{\hbar}{2} \frac{\sqrt{\pi}}{\Delta H(\beta)} C_{\text{ff}}(0), \tag{2.9a}$$

where

$$C_{\text{ff}}(0) = \left(\frac{\hbar}{2m}\right)^2 \frac{\partial^2}{\partial x_1 \partial x_2} (\langle x_2 | e^{-\beta \hat{H}/2} | x_1 \rangle)^2 = \left(\frac{\hbar}{2m}\right)^2 2 \langle x_1 | e^{-\beta \hat{H}/2} | x_2 \rangle' \langle x_2 | e^{-\beta \hat{H}/2} | x_1 \rangle. \tag{2.9b}$$

Note that the $C_{\text{ff}}(0)$ is the zero time value of the flux–flux autocorrelation function as defined by Miller, Schwarz and Tromp,³⁶

$$C_{\text{ff}}(t) = \text{tr} [e^{-\beta \hat{H}/2} \hat{F}_1 e^{-\beta \hat{H}/2} e^{i\hat{H}t/\hbar} \hat{F}_2 e^{-i\hat{H}t/\hbar}], \tag{2.10}$$

generalized to the case of two separate dividing surfaces.

Equation (2.9) is the basic result of the quantum instanton approximation, with $\Delta H(\beta)$ given by Eq. (2.7d). Though the derivation has focused explicitly on the tunneling regime, it is interesting to see what this QI approximation gives for higher temperature when over-barrier dynamics is dominant. The prototype for this is the free particle, i.e., no barrier, and in this limit the two dividing surfaces merge to the same position, i.e., $x_2 \rightarrow x_1$ (as is also seen below for higher temperatures with a real barrier). The free particle matrix of the Boltzmann operator is readily known,

$$\langle x_2 | e^{-\beta \hat{H}/2} | x_1 \rangle = \left(\frac{m}{\pi\hbar^2\beta}\right)^{1/2} e^{-(m/\hbar^2\beta)(x_2-x_1)^2}, \tag{2.11}$$

and the calculation straightforward; for example, Eq. (2.9b) gives

$$C_{\text{ff}}(0) = 1/\pi(\hbar\beta)^2, \tag{2.12a}$$

and Eq. (2.7d) gives

$$\Delta H(\beta) = \sqrt{2}/\beta, \tag{2.12b}$$

so that the rate constant is

$$kQ_r = \frac{kT}{h} \sqrt{\frac{\pi}{2}}, \tag{2.12c}$$

which is seen to be qualitatively correct, though a factor of $\sqrt{\pi/2} \sim 1.25$ too large.

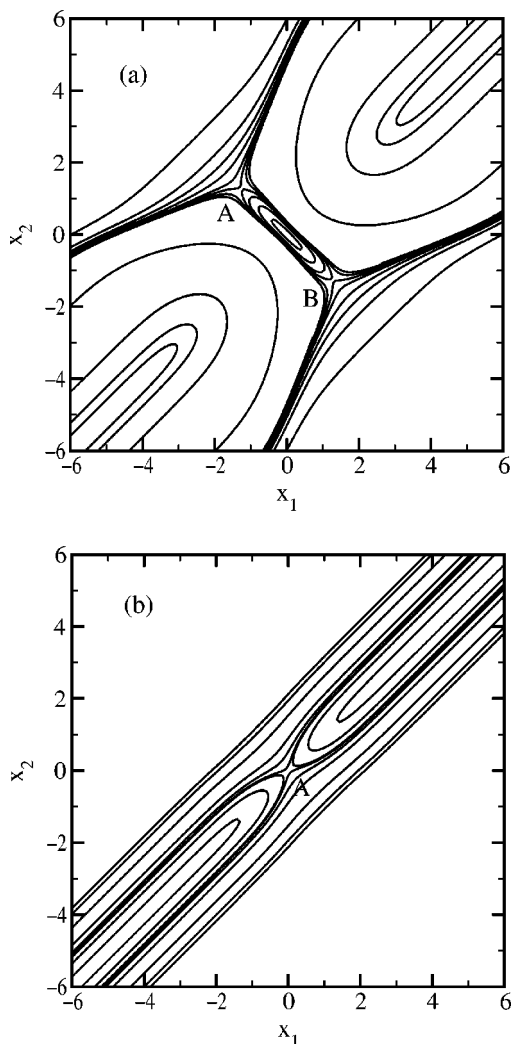


FIG. 1. A contour plot of the matrix element $\langle x_2 | \exp(-\beta\hat{H}/2) | x_1 \rangle$ in the 2D space (x_1, x_2) for the 1D symmetric Eckart barrier at temperature (a) $T = 100$ K, and (b) $T = 1000$ K. The two saddle points A and B in (a) merge into a single one at $x_1 = x_2 = 0$ in (b).

B. Results for the symmetric Eckart barrier

Before proceeding to the general multidimensional formulation it is useful to see how the QI approximation performs for a standard 1D barrier problem, the Eckart potential with parameters chosen to correspond approximately to the $\text{H} + \text{H}_2$ reaction; the potential function is

$$V(x) = V_0 \operatorname{sech}^2(ax), \quad (2.13)$$

with the parameters $V_0 = 0.425$ eV, $a = 1.36$ a.u. and $m = 1060$ a.u. The matrix elements of the Boltzmann operator needed in Eq. (2.7)–Eq. (2.9) (and elsewhere) are all evaluated in this paper by diagonalizing the Hamiltonian in a discrete variable basis. This is simpler for these low-dimensional examples than using Monte Carlo path integral methods, but this situation will be of course be reversed for systems with many degrees of freedom.

Figure 1 first shows contour plots of the matrix element $\langle x_2 | \exp(-\beta\hat{H}/2) | x_1 \rangle$ in the 2D space (x_1, x_2) , Fig. 1(a) for a

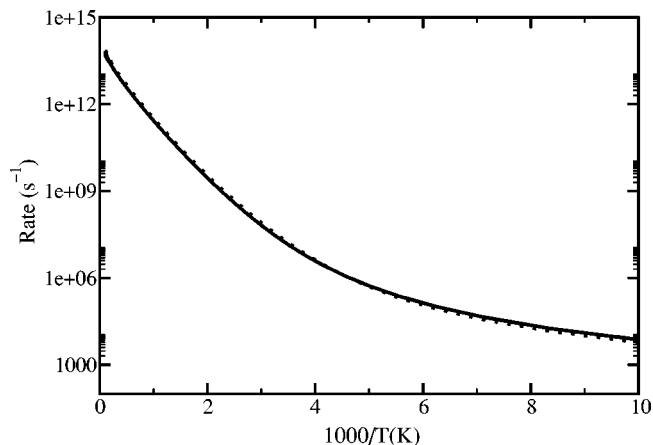


FIG. 2. An Arrhenius plot of the thermal rate constant for the 1D symmetric Eckart barrier. The solid curve is the exact result, and the dotted line the quantum instanton result.

low temperature (100 K) and Fig. 1(b) for a high temperature (1000 K). Because of the symmetry of the matrix element with respect to the interchange $x_1 \leftrightarrow x_2$, one can restrict attention to the upper half plane, $x_2 > 0$, but the plots are more esthetic in the full (x_1, x_2) space. It is clear that in this case of a symmetric potential barrier the two dividing surfaces are located symmetrically about the top of the barrier, i.e., $x_1 = -x_2$, with $x_1 < 0$ and $x_2 > 0$; this is point A in Fig. 1(a) (point B being the symmetrically equivalent point in the lower half plane). This point is a minimum along the coordinate $(x_1 + x_2)$ (because of the potential energy function) and a maximum along the coordinate $(x_1 - x_2)$ (the Franck–Condon maximum associated with the classical turning points of the imaginary time trajectory from x_1 to x_2); i.e., it is a *saddle point* in the 2D (x_1, x_2) space. At a higher temperature [Fig. 1(b)] these two saddle points merge into one: at $x_1 = x_2 = 0$, the conventional location of the two dividing surfaces at the top of the barrier.

Figure 2 shows an Arrhenius plot of the rate versus temperature over a broad range of temperature, but on this scale everything looks good! Therefore Fig. 3(a) plots the percent error of the QI result versus $1/T$. One sees that it describes the low temperature tunneling regime extremely well, and becomes $\sim 25\%$ too large at high temperature, as is understood from the discussion of the free particle limit above [cf. Eq. (2.12c)]. Figure 3(a) also shows the results obtained if one chooses the two dividing surfaces to be the same (at the top of the barrier) for all temperatures: at high temperature there is no difference (because the two dividing surfaces do in fact merge at high T); at low temperature, while it is not as good as utilizing two separate dividing surfaces, it is actually not too bad and has the advantage that it is easier to apply.

Finally, though $\sim 25\%$ error at high temperature is not so bad, one can easily correct for this in some *ad hoc* fashion. A way that we have found to be very simple and work well is to modify the factor $\Delta H(\beta)$ in Eq. (2.9a) as follows:

$$\Delta H_{\text{mod}}(\beta) = \Delta H(\beta) + \frac{\sqrt{\pi} - \sqrt{2}}{\beta}. \quad (2.14)$$

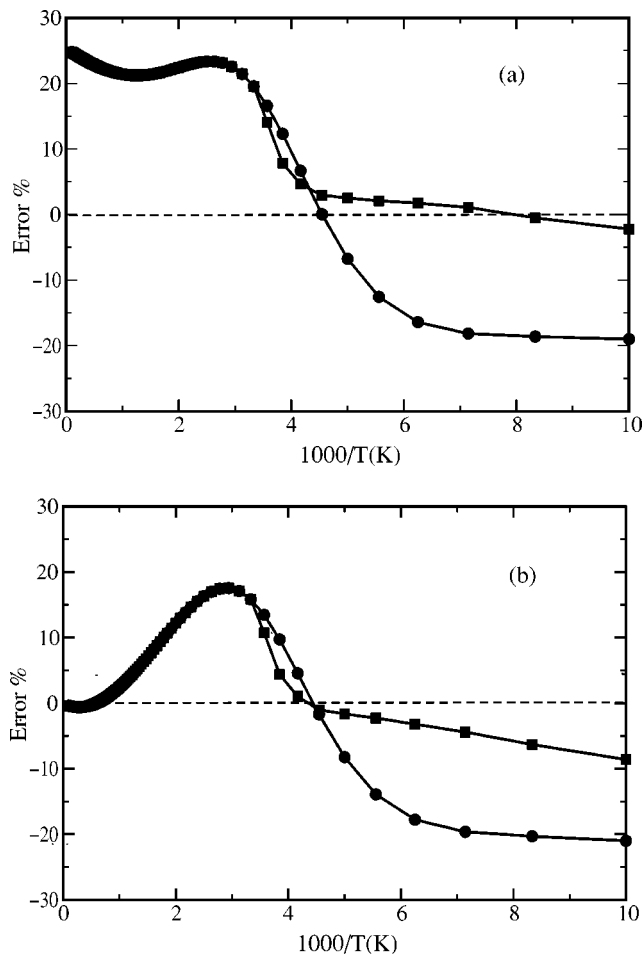


FIG. 3. Percent error ($100(k - k_{\text{exact}})/k_{\text{exact}}$) plot of the thermal rate constant for the quantum instanton approximation versus temperature for 1D symmetric Eckart barrier. Solid squares are the results with two dividing surfaces, and solid circles the results with a single dividing surface. (a) are the results using the original $\Delta H(\beta)$ [Eq. (2.7d)], and (b) the results using the modified $\Delta H(\beta)$ [Eq. (2.14)] that gives the correct high temperature limit.

This has very little effect in the low temperature regime, but at high temperature ΔH behaves as the free particle limit, Eq. (2.12b), so that Eq. (2.14) gives

$$\Delta H_{\text{mod}}(\beta) \approx \sqrt{\pi}/\beta, \quad (2.15)$$

which, when used in Eq. (2.9), gives the correct free particle (high T) limit. Figure 3(b) shows the percent error obtained using this modified ΔH factor, and one sees that with it the QI approximation provides quite good results for all temperatures.

C. Results for the asymmetric Eckart barrier

The second model system considered was the asymmetric Eckart barrier,³⁷

$$V(x) = \frac{V_0(1-\alpha)}{1 + e^{-2ax}} + \frac{V_0(1+\sqrt{\alpha})^2}{4 \cosh^2(ax)}, \quad (2.16)$$

where the parameters (a, m, V_0) were chosen to be the same as for the symmetric case, with the asymmetry parameter α

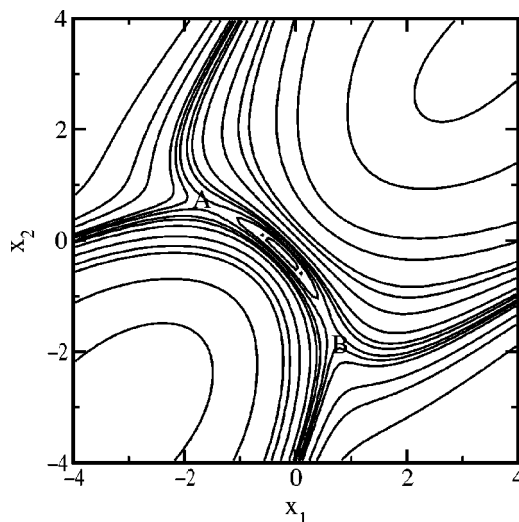


FIG. 4. A contour plot of matrix element $\langle x_2 | \exp(-\beta H/2) | x_1 \rangle$ in the 2D space (x_1, x_2) for the 1D asymmetric Eckart barrier at temperature $T = 100$ K.

$= 1.25$ chosen to give a $\sim 25\%$ difference between the barrier heights with respect to the left and right asymptotic regions.

Figure 4 first shows a contour plot of the Boltzmann operator matrix element $\langle x_2 | e^{-(\beta/2)H} | x_1 \rangle$ as a function of x_1 and x_2 for temperature $T = 100$ K. Saddle points (at positions A and B) are readily apparent, analogous to the symmetric case in Fig. 3(a), and determine the location of the two dividing surfaces; unlike the symmetric case, the two dividing surfaces are not located symmetrically, i.e., at $x_1 = -x_2$. The two saddle points merge into one at $T \approx 400$ K, a slightly higher transition temperature than for the analogous symmetric barrier.

Figure 5 shows the percent error given by the QI approximation for this asymmetric barrier (solid squares) and also the results (solid circles) obtained if one uses a single dividing surface. When using a single dividing surface we

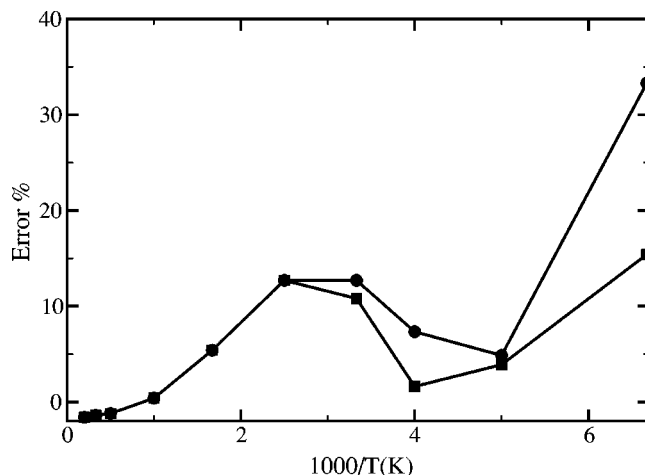


FIG. 5. Percent error of the thermal rate constant for the quantum instanton approximation versus temperature for 1D asymmetric Eckart barrier. Solid squares are the results with two dividing surfaces, and solid circles the results with one dividing surface.

choose the value $x_1 = x_2$ to be at the minimum on the contour plot in Fig. 4 (this is the minimum value of the diagonal matrix element $\langle x_1 | e^{\beta \hat{H}/2} | x_1 \rangle$) in order to satisfy the condition in Eq. (2.4). One sees that the QI approximation is essentially as accurate for this asymmetric barrier as it is for the symmetric one if one uses the (more accurate) version of the theory that employs two dividing surfaces. It is less accurate if one uses only a single dividing surface, a result that can be understood from the discussion in Appendix A following Eq. (A12).

D. The simplest QI approximation

An even simpler (but somewhat less accurate) quantum instantonlike approximation can be obtained by injecting some further semiclassical arguments into the development. We start with the QI result of Eq. (2.9) and use the SC approximation for matrix elements of the Boltzmann operator,¹⁷

$$\langle x_2 | e^{-\beta \hat{H}/2} | x_1 \rangle = \left[-\frac{\partial^2 S(x_2, x_1)}{\partial x_2 \partial x_1} / 2\pi\hbar \right]^{1/2} e^{-S(x_2, x_1)/\hbar}, \quad (2.17)$$

where $S(x_2, x_1)$ is the imaginary time action integral for the trajectory that goes from x_1 to x_2 in imaginary time $\hbar\beta/2$; with x_1 and x_2 chosen as in Sec. II A, there will be only one such trajectory. Derivatives of this matrix element, as needed in Eq. (2.9b), are evaluated in the usual SC spirit of differentiating only the action (exponent) of Eq. (2.17), so that Eq. (2.9) gives

$$kQ_r = \frac{\sqrt{\pi}}{\sqrt{-2E'(\beta)}} \left(\frac{\hbar}{2m} \right)^2 e^{-2S(x_2, x_1)/\hbar} \times \left(-\frac{\partial^2 S(x_2, x_1)}{\partial x_2 \partial x_1} \right)^2 / 2\pi\hbar. \quad (2.18)$$

Equation (2.18) is to be compared with the rate given by the original SC instanton approximation, which for one dimension is simply the Boltzmann average of the WKB tunneling probability,

$$kQ_r = \frac{1}{2\pi\hbar} \int dE e^{-\beta E} e^{-2S(E)/\hbar}, \quad (2.19a)$$

where $S(E)$ is the energy-dependent action integral from x_1 to x_2 ,

$$S(E) = \int_{x_1}^{x_2} dx \sqrt{2m[V(x) - E]}, \quad (2.19b)$$

and with the integral over E performed by the “stationary phase” approximation (cf. Appendix A). This gives

$$kQ_r = \frac{\sqrt{-2\pi E'(\beta)}}{2\pi\hbar} e^{-(\beta E + 2S(E)/\hbar)}, \quad (2.20a)$$

with $E = E(\beta)$ determined by the relation

$$\beta = -2S'(E)/\hbar \equiv \beta(E). \quad (2.20b)$$

If one now equates Eq. (2.18) and Eq. (2.20a), noting that the exponential factors are the same, this leads to the following SC relation:

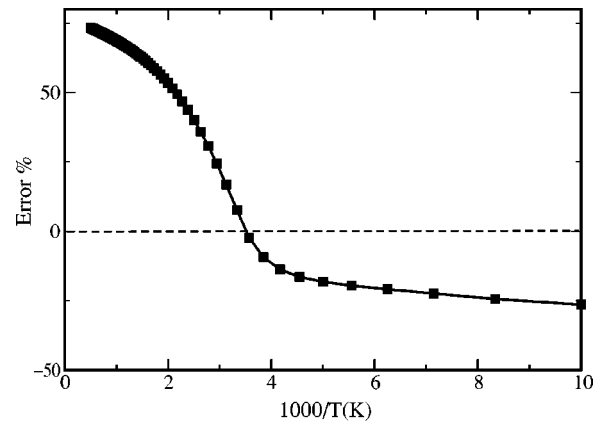


FIG. 6. Percent error of the thermal rate constant for the simplest quantum instanton (SQI) approximation of Eq. (2.22) versus temperature for a 1D symmetric Eckart barrier.

$$\frac{\hbar}{2m} \left(-\frac{\partial^2 S(x_2, x_1)}{\partial x_2 \partial x_1} \right) = \sqrt{-2E'(\beta)}. \quad (2.21)$$

Using this relation to eliminate the factor $\sqrt{-2E'(\beta)}$ in Eq. (2.18), and again making use of Eq. (2.17) to replace the SC matrix element by the quantum one, gives

$$kQ_r = \sqrt{\pi} \frac{\hbar}{2m} (\langle x_2 | e^{-\beta \hat{H}/2} | x_1 \rangle)^2, \quad (2.22a)$$

which involves only the (quantum) matrix element of the Boltzmann operator (and no derivatives thereof).

Equation (2.22) is our *simplest* quantum instanton (SQI) approximation. Its multidimensional generalization is apparent,

$$kQ_r = \sqrt{\pi} \frac{\hbar}{2m} \int d\mathbf{Q}_2 d\mathbf{Q}_1 (\langle x_2 \mathbf{Q}_2 | e^{-\beta \hat{H}/2} | x_1 \mathbf{Q}_1 \rangle)^2, \quad (2.22b)$$

which clearly has the correct separable limit (cf. the discussion in Sec. III).

Again, all of this development pertains to the low temperature tunneling regime, but it is nevertheless interesting to see how the result behaves in the free particle (i.e., high T) limit. Using Eq. (2.11), it is easy to show that Eq. (2.22a) gives

$$kQ_r = \sqrt{\pi} \frac{kT}{h}, \quad (2.23)$$

which is again seen to be qualitatively correct, but a factor of $\sqrt{\pi} \sim 1.77$ too large. [The SC instanton result, Eq. (2.20), is completely inapplicable for temperature T above the “crossover” temperature T_c , defined by $kT_c = \hbar \omega_b / 2\pi$, ω_b being the barrier frequency.]

Figure 6 shows the percent error given by this SQI approximation, Eq. (2.22a), for the same Eckart barrier as treated in Fig. 3. One sees that it is too large at high T [as understood by the free particle limit, Eq. (2.23)], and it also becomes too small at the lowest temperatures. Though not as accurate as the QI expression of Eq. (2.9), the SQI approximation of Eq. (2.22) is certainly easier to apply and is of useful accuracy. (It would look almost “exact” in an Arrhen-

ius plot like Fig. 2!) One could also experiment with various *ad hoc* modifications to correct the high T limit.

III. MULTIDIMENSIONAL GENERALIZATION

A. Derivation

We now consider a multidimensional system characterized by a reaction coordinate x and coordinates \mathbf{Q} orthogonal to it. If one proceeds in precisely the same manner as in Sec. II A, then one obtains the following expression for the rate constant:

$$kQ_r = \hbar \sqrt{\pi} \left(\frac{\hbar}{2m} \right)^2 \int d\mathbf{Q}_1 \int d\mathbf{Q}_2 \times [\langle x_1 \mathbf{Q}_1 | e^{-\beta \hat{H}/2} | x_2 \mathbf{Q}_2 \rangle \langle x_2 \mathbf{Q}_2 | e^{-\beta \hat{H}/2} | x_1 \mathbf{Q}_1 \rangle - \langle x_1 \mathbf{Q}_1 | e^{-\beta \hat{H}/2} | x_2 \mathbf{Q}_2 \rangle \langle x_2 \mathbf{Q}_2 | e^{-\beta \hat{H}/2} | x_1 \mathbf{Q}_1 \rangle] / \Delta H(\beta; \mathbf{Q}_1, \mathbf{Q}_2), \tag{3.1}$$

where again the primes indicate differentiation with respect to x_1 and x_2 , and

$$\Delta H(\beta; \mathbf{Q}_1, \mathbf{Q}_2)^2 = -2 \frac{\partial}{\partial \beta} E(\beta; \mathbf{Q}_1, \mathbf{Q}_2) \tag{3.2a}$$

$$= 4 \frac{\partial^2}{\partial \beta^2} \log \langle x_2 \mathbf{Q}_2 | e^{-\beta \hat{H}/2} | x_1 \mathbf{Q}_1 \rangle = \frac{\langle x_2 \mathbf{Q}_2 | e^{-\beta \hat{H}/2} \hat{H}^2 | x_1 \mathbf{Q}_1 \rangle}{\langle x_2 \mathbf{Q}_2 | e^{-\beta \hat{H}/2} | x_1 \mathbf{Q}_1 \rangle} - \left(\frac{\langle x_2 \mathbf{Q}_2 | e^{-\beta \hat{H}/2} \hat{H} | x_1 \mathbf{Q}_1 \rangle}{\langle x_2 \mathbf{Q}_2 | e^{-\beta \hat{H}/2} | x_1 \mathbf{Q}_1 \rangle} \right)^2. \tag{3.2b}$$

This result, however, is not completely satisfactory, on two grounds: one practical and one more fundamental. The practical problem is as follows: in applications to “real” molecular systems one will be evaluating the matrix elements of the Boltzmann operator in Eq. (3.1) by Monte Carlo path integration, and the integration over the (many) coordinates \mathbf{Q}_1 and \mathbf{Q}_2 will also have to be performed by Monte Carlo; the structure of Eq. (3.1) is that one would first have to perform the Monte Carlo path integration to obtain the matrix elements $\langle x_2 \mathbf{Q}_2 | \exp(-\beta \hat{H}/2) | x_1 \mathbf{Q}_1 \rangle$ for each set of coordinates $(\mathbf{Q}_1, \mathbf{Q}_2)$, and then perform the Monte Carlo integration over \mathbf{Q}_1 and \mathbf{Q}_2 ; i.e., one would have to perform a “Monte Carlo inside a Monte Carlo,” a very inefficient procedure. It would be much more efficient to be able to perform the Monte Carlo path integration and Monte Carlo integration over \mathbf{Q}_1 and \mathbf{Q}_2 simultaneously.

The more fundamental shortcoming of Eqs. (3.1)–(3.2) is that it is not correct in the separable limit, i.e., the case that the reaction coordinate x is uncoupled from the orthogonal coordinates \mathbf{Q} . In this limit the Hamiltonian is of the form

$$\hat{H} = \hat{h} + \hat{H}_b, \tag{3.3a}$$

where \hat{h} and H_b involve only the x and \mathbf{Q} degrees of freedom, respectively, and it is easy to see that the rate should

simply be the 1D rate constant for the x degree of freedom multiplied by the partition function Q_b for the \mathbf{Q} degrees of freedom,

$$Q_b = \text{tr}(e^{-\beta \hat{H}_b}). \tag{3.3b}$$

In the separable limit, however, Eq. (3.1) becomes

$$kQ_r = \hbar \sqrt{\pi} \left(\frac{\hbar}{2m} \right)^2 [\langle x_1 | e^{-\beta \hat{h}/2} | x_2 \rangle \langle x_2 | e^{-\beta \hat{h}/2} | x_1 \rangle - \langle x_1 | e^{-\beta \hat{h}/2} | x_2 \rangle \langle x_2 | e^{-\beta \hat{h}/2} | x_1 \rangle] \cdot \int d\mathbf{Q}_1 \int d\mathbf{Q}_2 (\langle \mathbf{Q}_2 | e^{-\beta \hat{H}_b/2} | \mathbf{Q}_1 \rangle)^2 / [\Delta h(\beta)^2 + \Delta H_b(\beta; \mathbf{Q}_1, \mathbf{Q}_2)^2]^{1/2}, \tag{3.4}$$

where we have used the fact that in the separable limit Eq. (3.2) gives $\Delta H(\beta; \mathbf{Q}_1, \mathbf{Q}_2)$ as

$$\Delta H(\beta; \mathbf{Q}_1, \mathbf{Q}_2)^2 = \Delta h(\beta)^2 + \Delta H_b(\beta; \mathbf{Q}_1, \mathbf{Q}_2)^2, \tag{3.5}$$

where

$$\Delta h(\beta)^2 = \frac{\langle x_2 | e^{-\beta \hat{h}/2} \hat{h}^2 | x_1 \rangle}{\langle x_2 | e^{-\beta \hat{h}/2} | x_1 \rangle} - \left(\frac{\langle x_2 | e^{-\beta \hat{h}/2} \hat{h} | x_1 \rangle}{\langle x_2 | e^{-\beta \hat{h}/2} | x_1 \rangle} \right)^2, \tag{3.6a}$$

$$\Delta H_b(\beta; \mathbf{Q}_1, \mathbf{Q}_2)^2 = \frac{\langle \mathbf{Q}_2 | e^{-\beta \hat{H}_b/2} \hat{H}_b^2 | \mathbf{Q}_1 \rangle}{\langle \mathbf{Q}_2 | e^{-\beta \hat{H}_b/2} | \mathbf{Q}_1 \rangle} - \left(\frac{\langle \mathbf{Q}_2 | e^{-\beta \hat{H}_b/2} \hat{H}_b | \mathbf{Q}_1 \rangle}{\langle \mathbf{Q}_2 | e^{-\beta \hat{H}_b/2} | \mathbf{Q}_1 \rangle} \right)^2. \tag{3.6b}$$

If one were to neglect the term ΔH_b^2 in Eq. (3.4), one would indeed obtain the correct separable limit, because

$$\int d\mathbf{Q}_1 \int d\mathbf{Q}_2 (\langle \mathbf{Q}_2 | e^{-\beta \hat{H}_b/2} | \mathbf{Q}_1 \rangle)^2 = \text{tr}(e^{-\beta \hat{H}_b/2} e^{-\beta \hat{H}_b/2}) = \text{tr}(e^{-\beta \hat{H}_b}) = Q_b. \tag{3.7}$$

A less drastic approximation than simply neglecting ΔH_b^2 in Eq. (3.4) is to expand the square root to first order in this quantity

$$(\Delta h^2 + \Delta H_b^2)^{-1/2} = \frac{1}{\Delta h} - \frac{\Delta H_b^2}{2\Delta h^3}, \tag{3.8}$$

so that the relevant part of Eq. (3.4) becomes

$$\int d\mathbf{Q}_1 \int d\mathbf{Q}_2 (\langle \mathbf{Q}_2 | e^{-\beta \hat{H}_b/2} | \mathbf{Q}_1 \rangle)^2 / [\Delta h(\beta)^2 + \Delta H_b(\beta; \mathbf{Q}_1, \mathbf{Q}_2)^2]^{1/2} \approx \frac{Q_b}{\Delta h(\beta)} - \frac{1}{2\Delta h(\beta)^3} \int d\mathbf{Q}_1 \int d\mathbf{Q}_2 (\langle \mathbf{Q}_2 | e^{-\beta \hat{H}_b/2} | \mathbf{Q}_1 \rangle)^2 \times \Delta H_b(\beta; \mathbf{Q}_1, \mathbf{Q}_2)^2; \tag{3.9}$$

in light of Eq. (3.6b), the second term above is seen to be proportional to

$$\begin{aligned} & \int d\mathbf{Q}_1 \int d\mathbf{Q}_2 [\langle \mathbf{Q}_1 | e^{-\beta \hat{H}_b/2} \hat{H}_b^2 | \mathbf{Q}_2 \rangle \langle \mathbf{Q}_2 | e^{-\beta \hat{H}_b/2} | \mathbf{Q}_1 \rangle \\ & - (\langle \mathbf{Q}_2 | e^{-\beta \hat{H}_b/2} \hat{H}_b | \mathbf{Q}_1 \rangle)^2] \\ & = \text{tr}(e^{-\beta \hat{H}_b/2} \hat{H}_b^2 e^{-\beta \hat{H}_b/2}) - \text{tr}(e^{-\beta \hat{H}_b/2} \hat{H}_b e^{-\beta \hat{H}_b/2} \hat{H}_b) \\ & = 0. \end{aligned} \quad (3.10)$$

$$\begin{aligned} \langle \Delta H(\beta)^2 \rangle & \equiv \frac{\int d\mathbf{Q}_1 \int d\mathbf{Q}_2 (\langle x_2 \mathbf{Q}_2 | e^{-\beta \hat{H}/2} | x_1 \mathbf{Q}_1 \rangle)^2 \Delta H(\beta; \mathbf{Q}_1, \mathbf{Q}_2)^2}{\int d\mathbf{Q}_1 \int d\mathbf{Q}_2 (\langle x_2 \mathbf{Q}_2 | e^{-\beta \hat{H}/2} | x_1 \mathbf{Q}_1 \rangle)^2} \\ & = \frac{\int d\mathbf{Q}_1 \int d\mathbf{Q}_2 [\langle x_1 \mathbf{Q}_1 | e^{-\beta \hat{H}/2} \hat{H}^2 | x_2 \mathbf{Q}_2 \rangle \langle x_2 \mathbf{Q}_2 | e^{-\beta \hat{H}/2} | x_1 \mathbf{Q}_1 \rangle - (\langle x_2 \mathbf{Q}_2 | e^{-\beta \hat{H}/2} \hat{H} | x_1 \mathbf{Q}_1 \rangle)^2]}{\int d\mathbf{Q}_1 \int d\mathbf{Q}_2 (\langle x_2 \mathbf{Q}_2 | e^{-\beta \hat{H}/2} | x_1 \mathbf{Q}_1 \rangle)^2}. \end{aligned} \quad (3.11b)$$

In the separable limit it is easy to see that

$$\langle \Delta H(\beta)^2 \rangle = \Delta h(\beta)^2, \quad (3.12)$$

so that the correct result is obtained for the rate constant in this limit. And equally important, from a practical point of view, is that the structure of Eq. (3.11) is such that the Monte Carlo integration over \mathbf{Q}_1 and \mathbf{Q}_2 and the path integration for the Boltzmann operator can be carried out simultaneously.

To summarize the multidimensional form of the quantum instanton approximation, one first chooses x_1 and x_2 so that the point (x_1, x_2) is a saddle point of the quantity

$$\int d\mathbf{Q}_1 \int d\mathbf{Q}_2 (\langle x_2 \mathbf{Q}_2 | e^{-\beta \hat{H}/2} | x_1 \mathbf{Q}_1 \rangle)^2, \quad (3.13a)$$

$$\langle \Delta H(\beta)^2 \rangle = \frac{\int d\mathbf{Q}_1 \int d\mathbf{Q}_2 [\langle x_1 \mathbf{Q}_1 | e^{-\beta \hat{H}/2} \hat{H}^2 | x_2 \mathbf{Q}_2 \rangle \langle x_2 \mathbf{Q}_2 | e^{-\beta \hat{H}/2} | x_1 \mathbf{Q}_1 \rangle - (\langle x_2 \mathbf{Q}_2 | e^{-\beta \hat{H}/2} \hat{H} | x_1 \mathbf{Q}_1 \rangle)^2]}{\int d\mathbf{Q}_1 \int d\mathbf{Q}_2 (\langle x_2 \mathbf{Q}_2 | e^{-\beta \hat{H}/2} | x_1 \mathbf{Q}_1 \rangle)^2}. \quad (3.13d)$$

And as in Sec. II, we also add the following term to $\Delta H(\beta)$ in order to get the correct free particle (high T) limit:

$$\Delta H(\beta) \rightarrow \Delta H(\beta) + (\sqrt{\pi} - \sqrt{2})/\beta. \quad (3.13e)$$

A further justification for using this root mean square average for $\Delta H(\beta)$, i.e., Eq. (3.11), is obtained by the following more heuristic derivation. Thus consider the expression for the rate constant as the time integral of the flux-flux autocorrelation function of Eq. (2.10),³⁶ with the two dividing surfaces chosen to be the same,

$$kQ_r = \int_0^\infty dt C_{\text{ff}}(t), \quad (3.14)$$

with

That is, the first order contribution of ΔH_b vanishes, so that to this order the correct separable limit is obtained for the rate constant.

The above analysis suggests the following more useful and general way to accomplish the correct behavior in the separable limit: the quantity $\Delta H(\beta; \mathbf{Q}_1, \mathbf{Q}_2)$ in Eq. (3.1) is replaced by its root mean square, defined as follows:

$$\Delta H(\beta; \mathbf{Q}_1, \mathbf{Q}_2) \rightarrow \sqrt{\langle \Delta H(\beta)^2 \rangle} \equiv \Delta H(\beta), \quad (3.11a)$$

where

in the 2D (x_1, x_2) space. Equation (3.1) then gives the rate constant as

$$\begin{aligned} kQ_r & = \frac{\hbar \sqrt{\pi}}{\Delta H(\beta)} \left(\frac{\hbar}{2m} \right)^2 \int d\mathbf{Q}_1 \int d\mathbf{Q}_2 [\langle x_1 \mathbf{Q}_1 | e^{-\beta \hat{H}/2} | x_2 \mathbf{Q}_2 \rangle \\ & \times \langle x_2 \mathbf{Q}_2 | e^{-\beta \hat{H}/2} | x_1 \mathbf{Q}_1 \rangle - \langle x_1 \mathbf{Q}_1 | e^{-\beta \hat{H}/2} | x_2 \mathbf{Q}_2 \rangle \\ & \times \langle x_2 \mathbf{Q}_2 | e^{-\beta \hat{H}/2} | x_1 \mathbf{Q}_1 \rangle], \end{aligned} \quad (3.13b)$$

with

$$\Delta H(\beta) = \sqrt{\langle \Delta H(\beta)^2 \rangle}, \quad (3.13c)$$

where

$$C_{\text{ff}}(t) = \text{tr}[e^{-\beta \hat{H}/2} \hat{F} e^{-\beta \hat{H}/2} e^{i(\hat{H}t/\hbar)} \hat{F} e^{-i(\hat{H}t/\hbar)}]. \quad (3.15)$$

[The flux operator \hat{F} involves only the reaction coordinate x and is given by Eq. (2.2) above.] With a short time approximation for the correlation function (which is consistent with transition state theory dynamics),

$$C_{\text{ff}}(t) = C_{\text{ff}}(0) + \ddot{C}_{\text{ff}}(0)t^2/2, \quad (3.16)$$

which is then exponentiated (i.e., a second order cumulative approximation),

$$C_{\text{ff}}(t) = C_{\text{ff}}(0) \exp\left[\frac{t^2}{2} \ddot{C}_{\text{ff}}(0)/C_{\text{ff}}(0)\right]. \quad (3.17)$$

Equation (3.14) gives

$$kQ_r = C_{\text{ff}}(0) \frac{1}{2} \left(\frac{2\pi C_{\text{ff}}(0)}{-\dot{C}_{\text{ff}}(0)} \right)^{1/2}, \quad (3.18)$$

i.e., the same as Eq. (2.9a) if we define $\Delta H(\beta)$ here by

$$\Delta H(\beta) = \hbar [-\dot{C}_{\text{ff}}(0)/2C_{\text{ff}}(0)]^{1/2}. \quad (3.19)$$

It is straightforward to evaluate the second derivative,

$$\begin{aligned} \ddot{C}_{\text{ff}}(0) = & -\frac{2}{\hbar^2} [\text{tr}(\hat{F}e^{-\beta\hat{H}/2}\hat{F}e^{-\beta\hat{H}/2}\hat{H}^2) \\ & - \text{tr}(\hat{F}e^{-\beta\hat{H}/2}\hat{H}\hat{F}e^{-\beta\hat{H}/2}\hat{H})], \end{aligned} \quad (3.20)$$

so that Eq. (3.19) becomes

$$\begin{aligned} \Delta H(\beta)^2 = & \frac{\text{tr}(\hat{F}e^{-\beta\hat{H}/2}\hat{F}e^{-\beta\hat{H}/2}\hat{H}^2) - \text{tr}(\hat{F}e^{-\beta\hat{H}/2}\hat{H}\hat{F}e^{-\beta\hat{H}/2}\hat{H})}{\text{tr}(\hat{F}e^{-\beta\hat{H}/2}\hat{F}e^{-\beta\hat{H}/2})}. \end{aligned} \quad (3.21)$$

[Interestingly, if Eq. (3.21) is used for the 1D Eckart barrier calculations of Sec. II, the results obtained for the rate constant in the low T tunneling regime are essentially unchanged from those presented there. In the high T , free particle limit, Eq. (3.21) gives $kQ_r = (kT/h)\sqrt{\pi/6}$, i.e., a fractional error

$\sim 28\%$ too small.] Equation (3.1), with the root mean square, Eq. (3.11) for $\Delta H(\beta)$ is then obtained by replacing the flux operator \hat{F} by the delta function $\delta(x-x_1)$, i.e., by assuming that the velocity factors cancel out between the numerator and denominator.

It is also useful to note the multidimensional expression for the case the reaction coordinate is defined as some general function of the coordinates of the system. Thus suppose \mathbf{q} denotes all the (Cartesian) coordinates of the system, and the reactant and product dividing surfaces are defined by the following equations:

$$s_1(\mathbf{q}) - s_1 = 0, \quad (3.22a)$$

$$s_2(\mathbf{q}) - s_2 = 0, \quad (3.22b)$$

respectively, where $s_1(\mathbf{q})$ and $s_2(\mathbf{q})$ are some specified functions of the coordinates. The flux operator \hat{F}_n in this case is

$$\begin{aligned} \hat{F}_n = & \frac{1}{2m} \left[\delta(s_n(\mathbf{q}) - s_n) \frac{\partial s_n(\mathbf{q})}{\partial \mathbf{q}} \cdot \hat{\mathbf{p}} \right. \\ & \left. + \hat{\mathbf{p}} \cdot \frac{\partial s_n(\mathbf{q})}{\partial \mathbf{q}} \delta(s_n(\mathbf{q}) - s_n) \right], \end{aligned} \quad (3.23)$$

where for simplicity it has been assumed that the mass m is the same for all Cartesian coordinates. Eq. (2.9a) for the rate constant still applies, here with

$$\begin{aligned} C_{\text{ff}}(0) = & 2 \left(\frac{\hbar}{2m} \right)^2 \int d\mathbf{q}_1 \int d\mathbf{q}_2 \delta(s_1(\mathbf{q}) - s_1) \delta(s_2(\mathbf{q}) - s_2) \times \\ & \left[\langle \mathbf{q}_1 | e^{-\beta\hat{H}/2} | \mathbf{q}_2 \rangle \left(\frac{\partial s_1(\mathbf{q}_1)}{\partial \mathbf{q}_1} \cdot \frac{\partial}{\partial \mathbf{q}_1} \frac{\partial s_2(\mathbf{q}_2)}{\partial \mathbf{q}_2} \cdot \frac{\partial}{\partial \mathbf{q}_2} \right) \right. \\ & \left. \times \langle \mathbf{q}_2 | e^{-\beta\hat{H}/2} | \mathbf{q}_1 \rangle - \left(\frac{\partial s_1(\mathbf{q}_1)}{\partial \mathbf{q}_1} \cdot \frac{\partial}{\partial \mathbf{q}_1} \right) \langle \mathbf{q}_1 | e^{-\beta\hat{H}/2} | \mathbf{q}_2 \rangle \left(\frac{\partial s_2(\mathbf{q}_2)}{\partial \mathbf{q}_2} \cdot \frac{\partial}{\partial \mathbf{q}_2} \right) \langle \mathbf{q}_2 | e^{-\beta\hat{H}/2} | \mathbf{q}_1 \rangle \right] \end{aligned} \quad (3.24a)$$

and

$$\Delta H(\beta)^2 = \frac{\int d\mathbf{q}_1 \int d\mathbf{q}_2 \delta(s_1(\mathbf{q}) - s_1) \delta(s_2(\mathbf{q}) - s_2) [\langle \mathbf{q}_1 | e^{-\beta\hat{H}/2} | \mathbf{q}_2 \rangle \langle \mathbf{q}_2 | e^{-\beta\hat{H}/2} | \mathbf{q}_1 \rangle - (\langle \mathbf{q}_1 | e^{-\beta\hat{H}/2} | \mathbf{q}_2 \rangle)^2]}{\int d\mathbf{q}_1 \int d\mathbf{q}_2 \delta(s_1(\mathbf{q}) - s_1) \delta(s_2(\mathbf{q}) - s_2) (\langle \mathbf{q}_1 | e^{-\beta\hat{H}/2} | \mathbf{q}_2 \rangle)^2}. \quad (3.24b)$$

In practice, the delta functions $\delta(s_n(\mathbf{q}) - s_n)$ can be replaced by finite representations, e.g.,

$$\delta(s_n(\mathbf{q}) - s_n) \rightarrow \left(\frac{\alpha}{\pi} \right)^{1/2} e^{-\alpha(s_n(\mathbf{q}) - s_n)^2}, \quad (3.25)$$

and a Monte Carlo procedure for evaluating the path integral for the Boltzmann operators $\exp(-\beta\hat{H}/2)$ and the integration over \mathbf{q}_1 and \mathbf{q}_2 simultaneously is then possible.

B. Application to the H+H₂ and D+H₂ reactions

Here we present results of the multidimensional version of the QI approximation for the collinear H+H₂ and D+H₂ reactions (on the LSTH^{38,39} potential energy surface). Matrix elements of the Boltzmann operator were calculated by diagonalizing the Hamiltonian matrix in a discrete variable representation using normal coordinates (x, Q) about the transition state.

Figure 7 shows contour plots of the potential energy surface for these two cases, also indicating the location of the two dividing surfaces at $T=200$ K [determined by finding the saddle points of the quantity in Eq. (3.13a)]. For temperatures above 300 K these two dividing surfaces merge into one. It is clear that two dividing surfaces are located symmetrically in the reactant and product regions for the H+H₂ case, while they are not symmetrically located for the asymmetric reaction D+H₂. All of these features are qualitatively similar to the one-dimensional examples discussed in Sec. II.

Rate constants were calculated from the multidimensional QI expressions summarized in Eq. (3.13), and Fig. 8 shows Arrhenius plots of the rate constant versus temperature (down to 150 K) for these two reactions. Again, to show in more detail the level of accuracy obtained by the QI approximation, Fig. 9 plots the percent error as a function of $1/T$, also showing the results obtained if one makes the ap-

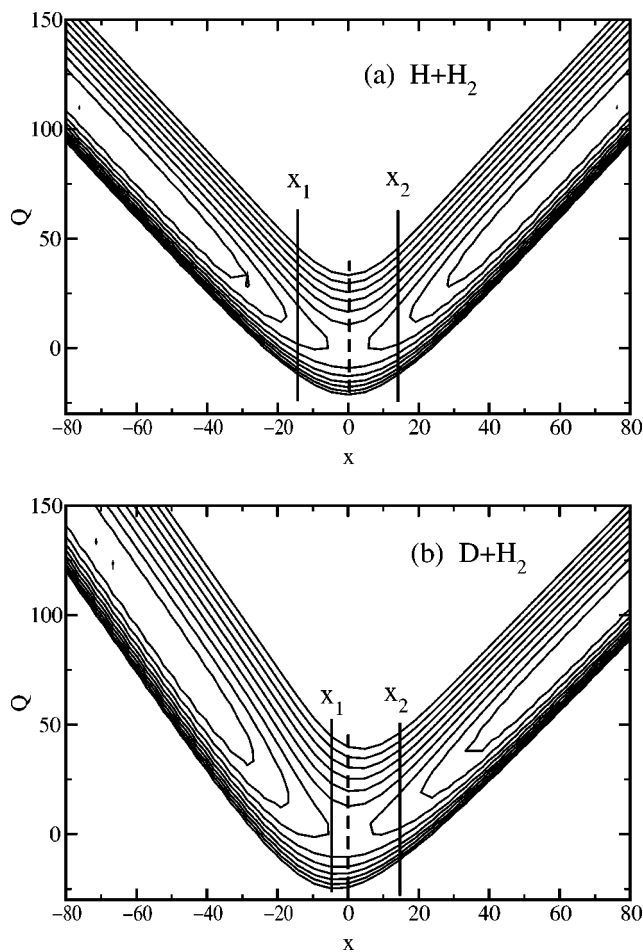


FIG. 7. Contour plots of the potential energy surfaces in transition state normal mode coordinates; the two dividing surfaces at x_1 and x_2 at $T = 200$ K are also indicated. (a) for $\text{H} + \text{H}_2$, and (b) for $\text{D} + \text{H}_2$.

proximation of using only one dividing surface at all temperatures. This latter, more approximate version of the theory is less accurate than the two-dividing-surface version, but it is simpler to apply. The more complete (two-dividing-surface version) of the QI approximation is seen to be correct to within 10% for the entire temperature range for both $\text{H} + \text{H}_2$ and $\text{D} + \text{H}_2$ reactions.

Examining the contour plots in Fig. 7 also suggests other variations for implementing the QI approximation. For example, one could vary the *angle* of the dividing surfaces in Fig. 7 (or even their shape); i.e., we have chosen only the simplest possibility for these test calculations—namely a straight line in transition state normal coordinates, but other choices might be better. The optimum shape of the dividing surfaces is a topic for future study.

IV. MICROCANONICAL RATE

Although one is interested in the thermal rate constant $k(T)$ in most applications, in some cases one would like to obtain the microcanonical rate as a function of total energy E , i.e., the cumulative reaction probability $N(E)$,

$$N(E) = \frac{1}{2} (2\pi\hbar)^2 \text{tr}[\hat{F}_1 \delta(E - \hat{H}) \hat{F}_2 \delta(E - \hat{H})]. \quad (4.1)$$

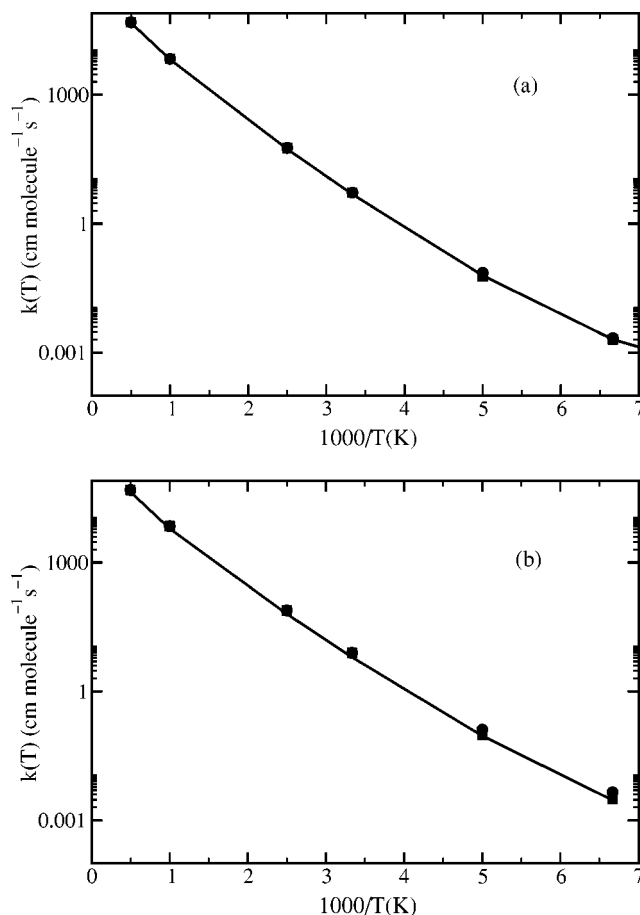


FIG. 8. Arrhenius plots of the thermal rate constant for the collinear (a) $\text{H} + \text{H}_2$ and (b) $\text{D} + \text{H}_2$ reactions, where the solid curve is the exact result, solid circles the results of the quantum instanton approximation with one dividing surface, and solid squares that with two dividing surfaces.

Furthermore, if one has obtained $N(E)$ for a sufficient range of energy E , it is of course possible to calculate $k(T)$ for a range of temperature T ,¹⁴

$$k(T) Q_r(T) = (2\pi\hbar)^{-1} \int dE e^{-\beta E} N(E). \quad (4.2)$$

It is therefore of interest to note explicitly the result for $N(E)$ given by the present quantum instanton approximation.

The development in Sec. II, i.e., Eqs. (2.3)–(2.7), gives $N(E)$ most conveniently in parametric form as follows:

$$N(E) = 2\pi \left(\frac{\hbar^2}{2m} \right)^2 [-2E'(\beta)]^{-1} \times e^{\beta E} \langle x_1 | e^{-\beta \hat{H}/2} | x_2 \rangle' \langle x_2 | e^{-\beta \hat{H}/2} | x_1 \rangle, \quad (4.3a)$$

with $E(\beta)$ given by Eq. (2.7c),

$$E(\beta) = \langle x_2 | e^{-\beta \hat{H}/2} \hat{H} | x_1 \rangle / \langle x_2 | e^{-\beta \hat{H}/2} | x_1 \rangle. \quad (4.3b)$$

As one varies β over its range, $E(\beta)$ is given by Eq. (4.3b) and $N(E(\beta))$ by Eq. (4.3a), thereby mapping out $N(E)$ parametrically.

As before, Eq. (4.3) pertains explicitly to the tunneling regime, but it is interesting to see what it gives for high

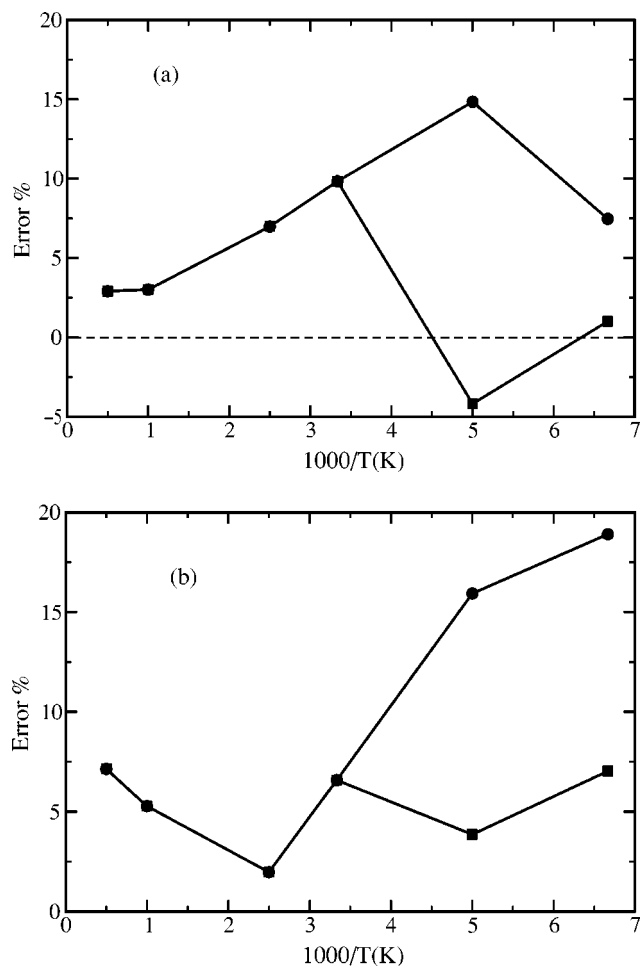


FIG. 9. Percent error for the thermal rate constant with the quantum instanton approximation versus temperature for (a) $\text{H}+\text{H}_2$ and (b) $\text{D}+\text{H}_2$ reactions. The solid circles are the results with one dividing surface, and the solid squares the results with two dividing surfaces.

energy E , i.e., the free particle limit. Utilizing Eq. (2.11), it is a simple calculation to show that in the free particle limit Eq. (4.3) gives

$$N(E) = \frac{e}{2} \approx 1.36, \quad (4.4)$$

whereas the correct result is of course $N(E) = 1$. One way to correct Eq. (4.3) to obtain the correct high energy limit is the following *ad hoc* modification to Eq. (4.3a),

$$-2E'(\beta) \rightarrow -2E'(\beta) + (e-2)/\beta^2. \quad (4.5)$$

One can also utilize the simplest quantum instanton (SQI) approximation described in Sec. IID to obtain a result for $N(E)$ that eliminates the need for derivatives with respect to x_1 and x_2 . Making use of Eq. (2.11) in Eq. (4.3), one obtains

$$N(E) = 2\pi \left(\frac{\hbar^2}{2m} \right) [-2E'(\beta)]^{-1/2} e^{\beta E} (\langle x_2 | e^{-\beta \hat{H}/2} | x_2 \rangle)^2, \quad (4.6)$$

with $E(\beta)$ still given by Eq. (4.3b). The free particle (high E) limit of Eq. (4.6) is

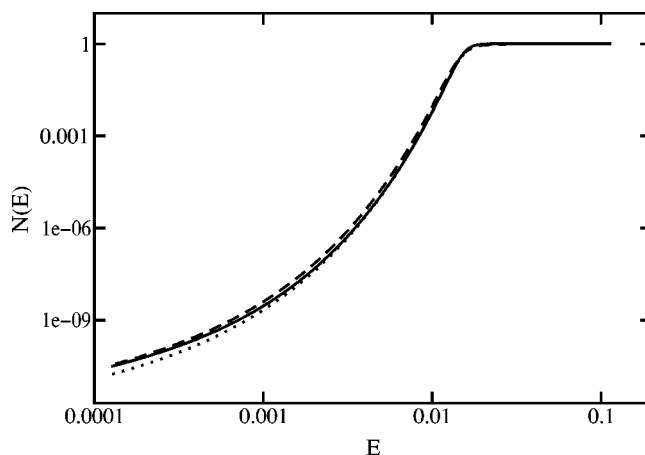


FIG. 10. Plots of the cumulative reaction probability versus energy. The solid line is the result for exact quantum mechanics, the dashed line the result for the quantum instanton approximation, and the dotted line the result for the simplest quantum instanton approximation.

$$N(E) = \frac{e}{\sqrt{2}} \approx 1.92, \quad (4.7)$$

thus suggesting the following *ad hoc* modification of Eq. (4.6) to obtain the correct high E limit:

$$\sqrt{-2E'(\beta)} \rightarrow \sqrt{-2E'(\beta)} + (e - \sqrt{2})/\beta. \quad (4.8)$$

Figure 10 shows the results for $N(E)$ given by the QI approximation [Eq. (4.3) with the modification of Eq. (4.5)] and the SQI approximation [Eq. (4.6) with the modification of Eq. (4.8)]. One sees very good agreement with the exact quantum results over the whole energy region, particularly so for the QI approximation.

V. CONCLUDING REMARKS

The original (semiclassical) instanton theory, involving a periodic orbit in imaginary time, only provides a description of the reaction rate in the tunneling regime (below the “cross over” temperature^{16,23}). The quantum generalization that has been developed in Sec. II (and its multidimensional generalization in Sec. III) describes the high temperature regime as well as providing a quantitative description of the tunneling regime. Like its SC predecessor, this quantum instanton (QI) theory involves only properties of the (quantum) Boltzmann operator. Since Monte Carlo path integral methods make it possible to compute the quantum Boltzmann operator for quite complex molecular systems, we believe that this QI approximation is a useful step toward providing a quantitative way of calculating rate constants for chemical reactions in complex systems.

The examples treated herein show the QI approximation (with a simple correction for the high temperature limit) to provide very good results (~ 10 – 20%) for the entire temperature range, for asymmetric as well as symmetric barriers. Applications to more complex systems are of course necessary to validate this performance more generally, and these are of course planned.

ACKNOWLEDGMENTS

This work has been supported by the Director, Office of Science, Office of Basic Energy Sciences, Chemical Sciences Division of the U.S. Department of Energy under Contract No. DE-AC03-76SF00098, and by National Science Foundation Grant No. CHE-0096576.

APPENDIX A: STEEPEST DESCENT RELATION BETWEEN $\delta(E - \hat{H})$ AND $\text{EXP}(-\beta \hat{H})$

The general form of the steepest descent approximation for an integral of the following type is

$$\int d\beta e^{-A(\beta)} \approx \left(\frac{2\pi}{A''(\beta_0)} \right)^{1/2} e^{-A(\beta_0)}, \quad (\text{A1})$$

where β_0 is the value of β for which $A'(\beta) = 0$. Applying this to Eq. (2.6), one has

$$A(\beta) = -\frac{\beta E}{2} - \log \langle x_2 | e^{-\beta \hat{H}/2} | x_1 \rangle, \quad (\text{A2})$$

so that

$$A'(\beta) = -\frac{E}{2} + \frac{1}{2} \langle x_2 | e^{-\beta \hat{H}/2} \hat{H} | x_1 \rangle / \langle x_2 | e^{-\beta \hat{H}/2} | x_1 \rangle, \quad (\text{A3})$$

and

$$A''(\beta) = \frac{1}{2} E'(\beta), \quad (\text{A4})$$

where $E(\beta)$ is defined by

$$E(\beta) = \langle x_2 | e^{-\beta \hat{H}/2} \hat{H} | x_1 \rangle / \langle x_2 | e^{-\beta \hat{H}/2} | x_1 \rangle. \quad (\text{A5})$$

The steepest descent value β_0 is thus the root of the equation

$$E = E(\beta). \quad (\text{A6})$$

The steepest descent approximation for Eq. (2.6) thus becomes

$$\begin{aligned} \langle x_2 | \delta(E - \hat{H}) | x_1 \rangle \\ = \frac{1}{4\pi i} \left(\frac{2\pi}{E'(\beta_0)/2} \right)^{1/2} e^{\beta_0 E/2} \langle x_2 | e^{-\beta_0 \hat{H}/2} | x_1 \rangle, \end{aligned} \quad (\text{A7})$$

or

$$\langle x_2 | \delta(E - \hat{H}) | x_1 \rangle = \frac{1}{\sqrt{2\pi \Delta H(\beta_0)}} e^{\beta_0 E/2} \langle x_2 | e^{-\beta_0 \hat{H}/2} | x_1 \rangle, \quad (\text{A8})$$

with

$$\Delta H(\beta) \equiv \sqrt{-2E'(\beta)}, \quad (\text{A9})$$

where $\beta_0(E)$ is determined by Eq. (A6). From Eq. (A5) one can also show that

$$\Delta H(\beta)^2 = \frac{\langle x_2 | e^{-\beta \hat{H}/2} \hat{H}^2 | x_1 \rangle}{\langle x_2 | e^{-\beta \hat{H}/2} | x_1 \rangle} - \left(\frac{\langle x_2 | e^{-\beta \hat{H}/2} \hat{H} | x_1 \rangle}{\langle x_2 | e^{-\beta \hat{H}/2} | x_1 \rangle} \right)^2, \quad (\text{A10})$$

which is seen to be positive [so that the matrix element given by Eqs. (A7) or (A8) is real, as it should be].

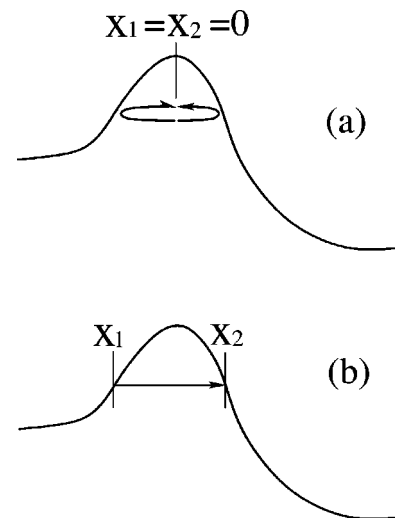


FIG. 11. A schematic depiction of the trajectories involved for different dividing surfaces in the semiclassical approximation: (a) corresponds to one dividing surface ($x_1 = x_2$) with two different trajectories, and (b) shows two dividing surfaces with only one trajectory from left turning point x_1 to right turning point x_2 .

The above discussion has dealt only with the quantum matrix elements of the Boltzmann operator, but it is illuminating to consider their semiclassical approximation,

$$\langle x_2 | e^{-\beta \hat{H}/2} | x_1 \rangle \approx C e^{-S(x_2, x_1; \hbar\beta/2)/\hbar}, \quad (\text{A11})$$

where S is the action integral along an imaginary time trajectory that goes from x_1 to x_2 in imaginary time $\hbar\beta/2$, and C is a pre-exponential factor that need not concern us here. Since the (imaginary) time derivative of S is the energy of the trajectory, the steepest descent condition of Eq. (A6) is simply that the energy E be the energy of this trajectory, i.e.,

$$E = \frac{2}{\hbar} \frac{\partial S}{\partial \beta}, \quad (\text{A12})$$

and the calculation then proceeds as above. For the $E \leftrightarrow \beta$ relation defined by Eq. (A12) to be uniquely defined, however, it is necessary that there be only *one* trajectory from x_1 to x_2 for a given E or β . For example, consider Fig. 11(a), corresponding to the choice $x_1 = x_2 = 0$; here there are two trajectories that go for 0 to 0—one that bounces off the left turning point and one off the right turning point (recall that motion in imaginary time is like that in real time on the inverted potential!). If the barrier is asymmetric, these two trajectories for energy E will take different amounts of (imaginary) time, or if one requires them to take the same time $\hbar\beta/2$, they will have different energies. In either event the $E \leftrightarrow \beta$ relation is not uniquely defined semiclassically. However, if x_1 and x_2 are chosen as in Fig. 11(b), namely at the left and right classical turning points, respectively, then there is only one trajectory from x_1 to x_2 at energy E or for (imaginary) time $\hbar\beta/2$. This is the reason for making the choice of x_1 and x_2 as in Eq. (2.4), i.e., at the Franck–Condon maxima, which is the quantum analog of their being at the classical turning points. Though this choice is motivated by semiclassical considerations, we see that it also

works best with the quantum Boltzmann operator. (At higher temperature, x_1 and x_2 merge to a common value.)

Finally, the steepest descent approximation is also used to evaluate the integral over energy in Eq. (2.8),

$$\int dE e^{-A(E)} = \left(\frac{2\pi}{A''(E_0)} \right)^{1/2} e^{-A(E_0)}, \quad (\text{A13})$$

where E_0 is the value determined by $A'(E) = 0$. For Eq. (2.8) one has

$$A(E) = \beta E - \beta_0(E)E - 2 \log \langle x_2 | e^{-\beta_0(E)\hat{H}/2} | x_1 \rangle, \quad (\text{A14})$$

so that

$$A'(E) = \beta - \beta_0(E) + \beta_0'(E)[-E + E(\beta_0(E))]; \quad (\text{A15})$$

however, since $E(\beta_0(E)) = E$, this becomes

$$A'(E) = \beta - \beta_0(E), \quad (\text{A16})$$

and then

$$A''(E) = -\beta_0'(E) = -1/E'(\beta_0), \quad (\text{A17})$$

and in light of Eq. (A9), this is also given by

$$A''(E) = 2/\Delta H(\beta_0(E))^2. \quad (\text{A18})$$

APPENDIX B: A MATHEMATICAL SUBTLETY

We would like to point out here a mathematical subtlety we encountered in the course of trying to obtain a quantum version of the instanton approximation. Our original intention had been to utilize Eq. (2.6) by writing a path integral expression for the Boltzmann operator, i.e.,

$$\begin{aligned} \langle x_N | e^{-(\beta/2)\hat{H}} | x_0 \rangle &= \int dx_1 \cdots \int dx_{N-1} \left(\frac{mN}{\pi\hbar^2\beta} \right)^{N/2} \\ &\times \exp \left[-\frac{m\Delta x^2}{\hbar^2\beta} - \frac{\beta}{2}\bar{V} \right], \end{aligned} \quad (\text{B1a})$$

where

$$\Delta x^2 = \sum_{k=1}^N (x_k - x_{k-1})^2, \quad (\text{B1b})$$

$$\bar{V} = \frac{1}{N} \left[\frac{1}{2} V(x_0) + \frac{1}{2} V(x_N) + \sum_{k=1}^{N-1} V(x_k) \right], \quad (\text{B1c})$$

and then interchange the order of the path integral and the integral over β ; with Eq. (B1) and this interchange, Eq. (2.6) for the matrix element of the density operator becomes

$$\begin{aligned} \langle x_N | \delta(E - \hat{H}) | x_0 \rangle &= \int dx_1 \cdots \int dx_{N-1} \frac{1}{4\pi i} \int d\beta \\ &\times \left(\frac{mN}{\pi\hbar^2\beta} \right)^{N/2} \exp \left[\frac{\beta E}{2} - \frac{m\Delta x^2}{\hbar^2\beta} - \frac{\beta}{2}\bar{V} \right]. \end{aligned} \quad (\text{B2})$$

(This is essentially what was done by one of us many years ago, using a Fourier path integral method; cf. the Appendix of Ref. 40.) If one now evaluates the integral over β by the steepest descent approximation of Appendix A (the conclu-

sions are unchanged if the integral is evaluated analytically, which is possible here), the exponent $A(\beta)$ for Eq. (A1) here is

$$A(\beta) = \frac{\beta}{2}(\bar{V} - E) + \frac{m\Delta x^2}{\hbar^2\beta}, \quad (\text{B3})$$

so that

$$A'(\beta) = \frac{1}{2}(\bar{V} - E) - \frac{m\Delta x^2}{\hbar^2\beta^2}, \quad (\text{B4a})$$

and then

$$A''(\beta) = \frac{2m\Delta x^2}{\hbar^2\beta^3}. \quad (\text{B4b})$$

The root of $A'(\beta) = 0$ is given by

$$\beta_0 = \frac{1}{\hbar} \left(\frac{2m\Delta x^2}{\bar{V} - E} \right)^{1/2}, \quad (\text{B4c})$$

and then

$$A(\beta_0) = \sqrt{2m\Delta x^2(\bar{V} - E)}/\hbar, \quad (\text{B5a})$$

$$A''(\beta_0) = \hbar(\bar{V} - E)^{3/2}/(2m\Delta x^2)^{1/2}. \quad (\text{B5b})$$

The exponent given by Eq. (B5a) seems entirely reasonable for the tunneling regime, where one has $\bar{V} - E > 0$. However, the quantity $A''(\beta)$ of Eq. (B5b) is positive, so that Eq. (B2) gives an *imaginary* result for matrix element of the density operator, rather than a real quantity (as it should be).

The problem arises because $A''(\beta)$ of Eq. (B5b) is positive. If the path integral were evaluated first, as is implicitly done in Appendix A, then the resulting $A''(\beta)$ for the steepest decent integral over β , Eq. (A4) is negative so that the result for the matrix element of $\delta(E - \hat{H})$ is real. This latter procedure has therefore been used for the development of the QI approximation in this paper.

This thus appears to be a situation where exchanging the order of integration—here that of the path integral and the integral over β —makes a difference!

¹H. Wang, X. Sun, and W. H. Miller, J. Chem. Phys. **108**, 9726 (1998).

²H. Eyring, J. Chem. Phys. **3**, 107 (1935).

³H. Eyring, Trans. Faraday Soc. **34**, 41 (1938).

⁴E. Wigner, Trans. Faraday Soc. **34**, 29 (1938).

⁵W. H. Miller, J. Chem. Phys. **61**, 1823 (1974).

⁶D. G. Truhlar, in *The Theory of Chemical Reaction Dynamics*, edited by M. Baer (CRC, Boca Raton, 1985), Vol. 4, Chap. 2.

⁷J. W. Tromp and W. H. Miller, J. Phys. Chem. **90**, 3482 (1986).

⁸(a) G. A. Voth, D. Chandler, and W. H. Miller, J. Chem. Phys. **91**, 7749 (1989). See also (b) S. Jang and G. A. Voth, *ibid.* **112**, 8747 (2000), for a more rigorous derivation of the centroid approach, and (c) E. Geva, Q. Shi, and G. A. Voth, *ibid.* **115**, 9209 (2001), for a generalization.

⁹G. A. Voth, Chem. Phys. Lett. **170**, 289 (1990).

¹⁰D. G. Truhlar and B. C. Garrett, J. Phys. Chem. **96**, 6515 (1992).

¹¹N. F. Hansen and H. C. Andersen, J. Chem. Phys. **101**, 6032 (1994).

¹²N. F. Hansen and H. C. Andersen, J. Phys. Chem. **100**, 1137 (1996).

¹³E. Pollak and J. L. Liao, J. Chem. Phys. **108**, 2733 (1998).

¹⁴W. H. Miller, J. Chem. Phys. **62**, 1899 (1975).

¹⁵S. Coleman, Phys. Rev. D **15**, 2929 (1977).

¹⁶A. J. Leggett, S. Chakravarty, A. T. Dosey, M. P. A. Fisher, A. Garg, and W. Zwerger, Rev. Mod. Phys. **59**, 1 (1987).

- ¹⁷W. H. Miller, *J. Chem. Phys.* **55**, 3146 (1971).
- ¹⁸E. M. Mortensen and K. S. Pitzer, *Chem. Soc. (London) Spec. Publ.* **16**, 57 (1962).
- ¹⁹R. A. Marcus, *J. Chem. Phys.* **45**, 4493 (1966).
- ²⁰E. A. McCullough and R. E. Wyatt, *J. Chem. Phys.* **54**, 3578 (1971).
- ²¹D. G. Truhlar and A. Kuppermann, *J. Chem. Phys.* **56**, 2232 (1972).
- ²²T. F. George and W. H. Miller, *J. Chem. Phys.* **57**, 2458 (1972).
- ²³P. Hanggi, P. Talkner, and M. Borkovec, *Rev. Mod. Phys.* **62**, 251 (1990).
- ²⁴V. A. Benderskii, V. I. Goldanskii, and D. E. Makarov, *Phys. Rep.* **233**, 195 (1993).
- ²⁵V. A. Benderskii, D. E. Makarov, and C. H. Wight, *Adv. Chem. Phys.* **88**, 1 (1994).
- ²⁶S. Chapman, B. C. Garrett, and W. H. Miller, *J. Chem. Phys.* **63**, 2710 (1975).
- ²⁷W. H. Miller, N. C. Handy, and J. E. Adams, *J. Chem. Phys.* **72**, 99 (1980).
- ²⁸D. G. Truhlar, B. C. Garrett, and S. J. Klippenstein, *J. Phys. Chem.* **100**, 12771 (1996).
- ²⁹A. Gonzalezlafont, S. N. Rai, G. C. Hancock, T. Joseph, and D. G. Truhlar, *Comput. Phys. Commun.* **75**, 143 (1993).
- ³⁰G. A. Voth, D. Chandler, and W. H. Miller, *J. Phys. Chem.* **93**, 7009 (1989).
- ³¹W. H. Miller, *J. Phys. Chem.* **103**, 9384 (1999).
- ³²(a) J. Shao, J. L. Liao, and E. Pollak, *J. Chem. Phys.* **108**, 9711 (1998). (b) J. L. Liao and E. Pollak, *J. Phys. Chem. A* **104**, 1799 (2000).
- ³³K. Yamashita and W. H. Miller, *J. Chem. Phys.* **82**, 5475 (1985).
- ³⁴G. Krilov, E. Sim, and B. J. Berne, *J. Chem. Phys.* **114**, 1075 (2001).
- ³⁵E. Sim, G. Krilov, and B. J. Berne, *J. Phys. Chem. A* **105**, 2824 (2001).
- ³⁶W. H. Miller, S. D. Schwartz, and J. W. Tromp, *J. Chem. Phys.* **79**, 4889 (1983).
- ³⁷H. S. Johnston, *Gas Phase Reaction Rate Theory* (Ronald, New York, 1966), pp. 37–47.
- ³⁸P. Siegbahn and B. Liu, *J. Chem. Phys.* **68**, 2457 (1978).
- ³⁹D. G. Truhlar and C. J. Horowitz, *J. Chem. Phys.* **68**, 2466 (1978).
- ⁴⁰W. H. Miller, *J. Chem. Phys.* **63**, 1166 (1975).